J|A|C|S ARTICLES

Published on Web 07/14/2010

Compositional Control of the Superconducting Properties of LiFeAs

Michael J. Pitcher,[†] Tom Lancaster,[‡] Jack D. Wright,[‡] Isabel Franke,[‡] Andrew J. Steele,[‡] Peter J. Baker,[§] Francis L. Pratt,[§] William Trevelyan Thomas,[†] Dinah R. Parker,[†] Stephen J. Blundell,*[,‡] and Simon J. Clarke*[,†]

Department of Chemistry, University of Oxford, Inorganic Chemistry Laboratory, South Parks Road, Oxford OX1 3QR, United Kingdom, Department of Physics, University of Oxford, Clarendon Laboratory, Parks Road, Oxford OX1 3PU, United Kingdom, and ISIS Facility, STFC-Rutherford Appleton Laboratory, Harwell Science and Innovation Campus, Didcot OX11 0QX, United Kingdom

Received April 15, 2010; E-mail: simon.clarke@chem.ox.ac.uk; stephen.blundell@physics.ox.ac.uk

Abstract: The response of the superconducting state and crystal structure of LiFeAs to chemical substitutions on both the Li and the Fe sites has been probed using high-resolution X-ray and neutron diffraction measurements, magnetometry, and muon-spin rotation spectroscopy. The superconductivity is extremely sensitive to composition: Li-deficient materials ($Li_{1-y}Fe_{1+y}As$ with Fe substituting for Li) show a very rapid suppression of the superconducting state, which is destroyed when y exceeds 0.02, echoing the behavior of the $Fe_{1+y}Se$ system. Substitution of Fe by small amounts of Co or Ni results in monotonic lowering of the superconducting transition temperature, T_c, and the superfluid stiffness, ρ_s, as the electron count increases. T_c is lowered monotonically at a rate of 10 K per 0.1 electrons added per formula unit irrespective of whether the dopant is Co and Ni, and at higher doping levels superconductivity is completely suppressed. These results and the demonstration that the superfluid stiffness in these LiFeAs-derived compounds is higher than in all of the iron pnictide materials underlines the unique position that LiFeAs occupies in this class.

Introduction

High temperature superconductivity, which is demonstrably unconventional in nature in most cases, seems to be ubiquitous in compounds containing FeAs anti-PbO-type (i.e., antifluorite-type) layers. LaFeAsO with the ZrSiCuAs structure type was found to superconduct below 26 K when doped with electrons through the substitution of about 10−20% of the oxide ions by fluoride.[1] The incorporation of an oxygen deficiency and the use of smaller lanthanides results in higher T_c's, and the highest T_c reported in this class is 55 K in $SmFeAsO_{1-x}F_x$[2] (derived from the onset of a rapid decrease in resistivity with decreasing temperature). These ZrSiCuAs-type superconductors are colloquially referred to as the "1111" compounds (to indicate the stoichiometry) and include the isostructural derivatives of AeFeAsF (Ae = Ca, Sr, Eu).[3−6] The best-studied iron pnictide superconductors are the "122" class with the common $ThCr_2Si_2$ structure type. These compounds, which are the most amenable to crystal growth, are exemplified by derivatives of $AEFe_2As_2$ (AE = Ca, Sr, Ba) obtained by hole-doping on the AE site (e.g., $Ba_{1-x}K_xFe_2As_2$, optimal $T_c = 38$ K for $x = 0.4$[7]) or electron doping on the Fe site (e.g., $Ba(Fe_{1-x}Co_x)_2As_2$, optimal $T_c = 22$ K for $x = 0.063$.[8]). The high T_c's and critical fields exhibited by these superconductors suggest that they are unconventional superconductors with properties that cannot be described within the framework of existing models of superconductivity such as the BCS theory. The proximal occurrence of itinerant antiferromagnetism and superconductivity in the phase diagram suggests that the pairing mechanism for superconductivity has a magnetic origin, although further measurements are required before a predictive theory of superconductivity will emerge.

Some of us,[9] in parallel with other groups,[10,11] recently described superconductivity at temperatures below 16 K in stoichiometric LiFeAs (formally Fe^{2+}) (Figure 1), a member of the "111" class of pnictide superconductor, which was first

[†] Department of Chemistry, University of Oxford.
[‡] Department of Physics, University of Oxford.
[§] ISIS Facility.

(1) Kamihara, Y.; Watanabe, T.; Hirano, M.; Hosono, H. *J. Am. Chem. Soc.* **2008**, *130*, 3296.
(2) Ren, Z. A.; Che, G. C.; Dong, X.-L.; Yang, J.; Lu, W.; Yi, W.; Shen, X.-L.; Li, Z.-C.; Sun, L.-L.; Zhou, F.; Zhao, Z.-X. *Europhys. Lett.* **2008**, *83*, 17002.
(3) Matsuishi, S.; Inoue, Y.; Nomura, T.; Yanagi, H.; Hirano, M.; Hosono, H. *J. Am. Chem. Soc.* **2008**, *130*, 14428.
(4) Tegel, M.; Johansson, S.; Weiss, V.; Schellenberg, I.; Hermes, W.; Pöttgen, R.; Johrendt, D. *Europhys. Lett.* **2008**, *84*, 67007.
(5) Han, F.; Zhu, X.; Mu, G.; Cheng, P.; Wen, H.-H. *Phys. Rev. B* **2008**, *78*, 180503(R).
(6) Zhu, X.; Han, F.; Cheng, P.; Mu, G.; Shen, B.; Fang, L.; Wen, H.-H. *Europhys. Lett.* **2009**, *85*, 17011.
(7) Rotter, M.; Tegel, M.; Johrendt, D. *Phys. Rev. Lett.* **2008**, *101*, 107006.
(8) Sefat, A. S.; Jin, R.; McGuire, M. A.; Sales, B. C.; Singh, D. J.; Mandrus, D. *Phys. Rev. Lett.* **2008**, *101*, 117004.
(9) Pitcher, M. J.; Parker, D. R.; Adamson, P.; Herkelrath, S. J. C.; Boothroyd, A. T.; Ibberson, R. M.; Brunelli, M.; Clarke, S. J. *Chem. Commun.* **2008**, 5918.
(10) Tapp, J. H.; Tang, Z.; Lv, B.; Sasmal, K.; Lorenz, B.; Chu, P. C. W.; Guloy, A. M. *Phys. Rev. B* **2008**, *78*, 060505.
(11) Wang, X. C.; Liu, Q. Q.; Lv, Y. X.; Gao, W. B.; Yang, L. X.; Yu, R. C.; Li, F. Y.; Jin, C. Q. *Solid State Commun.* **2008**, *148*, 538.

Figure 1. Anti-PbFCl-type crystal structure of LiFeAs. The sites are identified by their Wyckoff label. In the $Li_{1-y}Fe_{1+y}As$ series, Fe substitutes for Li on the 2*c* cation site, and in the $LiFe_{1-x}M_xAs$ series, M = Co,Ni are substituted for Fe on the 2*a* site.

synthesized in 1968.[12] We and others later showed that superconductivity was suppressed in LiFeAs on the application of hydrostatic pressure.[13,14] Furthermore, we have revealed strong interplay between antiferromagnetism and superconductivity, which exists in the Co-and Ni-doped derivatives of the isostructural antiferromagnet NaFeAs.[15,16]

LiFeAs shows behavior that contrasts with that of many of the other iron pnictide superconductors. First, a consequence of accommodating the small Li^+ ion between the FeAs layers is that the edge-staring $FeAs_4$ tetrahedra are extremely compressed in the basal plane. Second, superconductivity occurs in the stoichiometric material LiFeAs, whereas for the other iron arsenide superconductors doping away from the formal oxidation state of Fe^{2+} or the application of hydrostatic pressure is required to induce superconductivity. Contrary to one early report that superconductivity occurs in highly Li-deficient materials,[11] there is reliable evidence[9,10] that the superconductor is stoichiometric LiFeAs. Third, and in line with the fact that it is a bulk superconductor, stoichiometric LiFeAs does not appear to show static magnetism, in contrast to NaFeAs[15] and all of the known "122" and "1111" iron arsenides.

In this Article, we describe the response of the crystal structure and superconductivity of LiFeAs to two types of substitution. The first is doping of the Li-site by excess Fe to produce $Li_{1-y}Fe_{1+y}As$ phases: a type of doping that was first described in the original report by Juza and Langer[12] and that very rapidly destroys the superconducting state. The second type of doping is by Co and Ni on the Fe site to produce $LiFe_{1-x}M_xAs$ (M = Co, Ni); this suppresses superconductivity less rapidly than doping on the Li site and produces a series of superconductors, which we have probed using muon-spin rotation experiments to study the correlation of the superfluid stiffness with T_c and make comparisons with related superconductors.

Experimental Section

Synthesis. All manipulations of solids were carried out in a Glove Box Technology drybox containing recirculating argon with a combined O_2 and H_2O content of less than 5 ppm. We prepared several series of samples. First, 3 g powder samples $Li_{1-y}Fe_{1+y}As$ were prepared for values of *y* between 0.01 and 0.05: pieces of Li metal (Aldrich, 99.9%) were added to a well-ground mixture of Fe powder (Alfa, 99.998% used as received) and As powder (Alfa, 99.9999% pieces, ground under argon prior to use) and sealed in a niobium tube by arc-welding under a flow of argon. The reaction vessel was initially heated for 12 h at 220 °C. The resulting brown powder was then thoroughly reground and pelletized and annealed for 48 h at 800 °C in a sealed niobium tube contained within a protective evacuated silica envelope. In the analysis of these Li-poor/Fe-rich materials $Li_{1-y}Fe_{1+y}As$, we also consider "sample 2" from ref 9, which was evidently very close to stoichiometric according to diffraction measurements,[9] but which had a lower T_c than all of the other reported samples of LiFeAs.[9−11]

Second, we prepared samples of composition $LiFe_{1-x}Co_xAs$ and $LiFe_{1-x}Ni_xAs$. These were prepared in a way similar to the $Li_{1-y}Fe_{1+y}As$ series except that Co (Alfa 99.998%) or Ni (Alfa 99.996%) powders were substituted for some of the iron powder in the mixture of transition metals and arsenic. LiCoAs has been reported,[12] and Co-containing samples were successfully prepared single phase when the samples were removed from the furnace at high temperature and allowed to cool on the bench. LiNiAs has not been reported, and this may explain why Ni-doped samples were found to be more prone to phase separation, particularly for $x > 0.05$ with phase competition from NiAs, $FeAs_2$, Li_3As, and $Li_{3.2}Ni_{10.8}As_7$[17] evident from X-ray powder diffraction measurements. Single-phase Ni-doped samples with *x* up to 0.4 were attainable when the reactions were quenched rapidly to room temperature, so this protocol was adopted for all of the Ni-doped samples: the Nb reaction vessels were heated under a flow of argon for protection and then quenched by plunging them immediately into cold water on removal from the furnace. For this work, $LiFe_{1-x}Co_xAs$ were prepared with $x = 0.025$, 0.05, 0.075, 0.10, 0.15, and 0.20, and $LiFe_{1-x}Ni_xAs$ were prepared with $x = 0.005$, 0.01, 0.015, 0.02, 0.025, 0.05, 0.10, and 0.20. This range of compositions was found to be wide enough to encompass the superconducting domain of interest, and we do not consider samples richer in Co or Ni here. All of the samples considered appeared to be single phase by laboratory X-ray powder diffraction.

Structural Characterization. Laboratory X-ray powder diffraction (XRPD) to assess phase purity was carried out using a PANalytical X'Pert PRO instrument equipped with a Ge(111) monochromator and an X'cellerator multiangle detector. Cu $K\alpha_1$ radiation was used. Detailed structural characterization was carried out by complementary use of neutron powder diffraction (NPD) using the time-of-flight instruments HRPD and POLARIS at the ISIS Facility, UK, and synchrotron XRPD using beamline I11 at the Diamond Light Source, UK,[18,19] and beamline ID31 at the ESRF, France. For NPD measurements, the samples were contained in 6 mm diameter vanadium cylinders. On HRPD, data were collected using data banks at $2\theta = 90°$ and 168°, and on POLARIS, data banks were located at $2\theta = 35°$, 90°, and 145°. On I11, 0.8272 Å X-rays were used for the analysis of the $Li_{1-y}Fe_{1+y}As$ series, and 0.60095 Å X-rays were used for $LiFe_{1-x}Ni_xAs$ samples. Monochromatic X-rays were selected from the white beam using a liquid-nitrogen-cooled Si(111) monochromator and harmonic rejection mirrors, and the wavelength was calibrated using a Si standard. The samples were contained in 0.5 mm diameter borosilicate glass capillaries, and the patterns were recorded using five multianalyzer-crystal detectors. On ID31, 0.3994 Å X-rays were used for $LiFe_{1-x}Co_xAs$ samples with $x = 0.1$ and 0.2. We also consider LiFeAs "sample 2" from our earlier work, which was measured on HRPD and ID31 at ESRF as described previously.[9]

Magnetometry. Magnetic susceptibility measurements were made using a Quantum Design MPMS-XL SQUID magnetometer. The powder samples were immobilized in gelatin capsules.

(12) Juza, R.; Langer, K. *Z. Anorg. Allg. Chem.* **1968**, *361*, 58.
(13) Mito, M.; Pitcher, M. J.; Crichton, W.; Garbarino, G.; Baker, P. J.; Blundell, S. J.; Adamson, P.; Parker, D. R.; Clarke, S. J. *J. Am. Chem. Soc.* **2009**, *131*, 2986.
(14) Gooch, M.; Lv, B.; Tapp, J. H.; Tang, Z.; Lorenz, B.; Guloy, A. M.; Chu, P. C. W. *Europhys. Lett.* **2009**, *85*, 27005.
(15) Parker, D. R.; Pitcher, M. J.; Baker, P. J.; Franke, I.; Lancaster, T.; Blundell, S. J.; Clarke, S. J. *Chem. Commun.* **2009**, 2189.
(16) Parker, D. R.; Smith, M. J. P.; Lancaster, T.; Steele, A. J.; Franke, I.; Baker, P. J.; Pratt, F. L.; Pitcher, M. J.; Blundell, S. J.; Clarke, S. J. *Phys. Rev. Lett.* **2010**, *104*, 057007.
(17) Welzl, C.; Schuster, H. U. *Z. Kristallogr.* **1991**, *196*, 179.
(18) Tang, C. C.; Thompson, S. P.; Hill, T. P.; Wilkin, G. R.; Wagner, U. H. *Z. Kristallogr. Suppl.* **2007**, *26*, 153.
(19) Thompson, S. P.; Parker, J. E.; Potter, J.; Hill, T. P.; Birt, A.; Cobb, T. M.; Yuan, F.; Tang, C. C. *Rev. Sci. Instrum.* **2009**, *80*, 075107.

Measurements were made in DC fields of 10−50 Oe in the temperature range 2−300 K after cooling in zero applied field (zero-field-cooled: ZFC) and in the measuring field (field-cooled: FC). For superconducting samples, T_c was determined as the intercept between the extrapolation of the normal state susceptibility below T_c and the line coincident with the most rapidly changing susceptibility in the superconducting state.[13]

Muon-Spin Rotation Spectroscopy. Transverse-field muon-spin rotation (TF-μSR) experiments on the $LiFe_{1-x}M_xAs$ (M = Co, Ni) materials were carried out as follows: $LiFe_{0.975}Co_{0.025}As$ and $LiFe_{0.95}Co_{0.05}As$ were measured on the GPS instrument at SμS, Paul Scherrer Institut, Switzerland; $LiFe_{0.925}Co_{0.075}As$, $LiFe_{0.99}Ni_{0.01}As$, and $LiFe_{0.98}Ni_{0.02}As$ were measured on the MuSR instrument at ISIS, Rutherford Appleton Laboratory, UK. Samples of 0.5−1.0 g in mass were packed, in the argon-filled glovebox, into square Ag-foil packets (1−2 cm square, ∼25 μm foil thickness), which were crimped tightly closed. These sealed packets were only exposed to air very briefly during loading into the cryostat. TF-μSR is a method for accurately measuring the internal magnetic field distribution within the vortex lattice of a type-II superconductor.[20] Spin-polarized positive muons (gyromagnetic ratio $\gamma_\mu/2\pi = 135.5$ MHz T^{-1}; lifetime $\tau_\mu = 2.2$ μs) are implanted at random positions on the length scale of the vortex lattice. A magnetic field ($B_{c1} < B_{app} < B_{c2}$) is applied perpendicular to the initial muon spin direction, and the muon spins precess around the total local magnetic field at their stopping sites. The muon decays into a positron and two neutrinos, the former of which is detected, allowing the temporal evolution of the polarization to be measured. This in turn allows for the random sampling of the local field distribution $p(B)$ across the vortex lattice via its relationship with the spin polarization $P_x(t)$:

$$P_x(t) = \int_0^\infty p(B)\cos(\gamma_\mu B t + \phi)\,dB \qquad (1)$$

where ϕ is a phase offset associated with the detector geometry. The resulting field distribution $p(B)$ is related to the superfluid stiffness, ρ_s, which is the density of superconducting Cooper pairs divided by their effective mass. The in-plane penetration depth, λ_{ab}, is related to the superfluid stiffness by $\lambda_{ab} = (c/\rho_s)^{-0.5}$, where c is the speed of light.

Results and Discussion

$Li_{1-y}Fe_{1+y}As$ Samples. Structures. Juza and Langer[12] described the system $Li_{1-y}Fe_{1+y}As$ between the limits LiFeAs and Fe_2As. The anti-PbFCl structure is maintained for all members. The conclusion of their work was that the composition LiFeAs was not attainable, rather that a range of Li-rich samples was produced in the range $Li_{1.1-y}Fe_{1+y}As$ ($0 \le y \le 0.14$), and it was suggested that the additional metal atoms resided on additional 2*b* sites in the LiAs slabs of the structure. They described a phase gap between these Li-rich compounds close to LiFeAs and compounds close to Fe_2As with compositions $Li_xFe_{2-x}As$ ($0 \le x \le 0.25$) in which Li was substituted into Fe_2As. Our earlier work[9] using a combination of synchrotron XRPD and NPD showed, along with the work of others,[10] that the stoichiometric composition is attainable, that the 2*c* and 2*a* cation sites and the 2*c* anion site were fully occupied, that there was no Li/Fe disorder, and that the proposed additional 2*b* site for Li was not occupied within the experimental uncertainty. In the nonstoichiometric materials $Li_{1-y}Fe_{1+y}As$, the only realistic model has the extra Fe ions partially occupying the 2*c* site at the expense of some Li (see Figure 1). This is the site that is partially occupied in $Fe_{1+x}Te$, and that is fully occupied by Fe in Fe_2As. Neutrons are required to enable the light Li atom to be located accurately, but the use of neutrons alone is unsatisfactory when there is the possibility of Li/Fe disorder because the negative scattering length of Li (−1.90 versus 9.54 fm for Fe) means a site-sharing $Li_{0.97}Fe_{1.03}As$ model is essentially indistinguishable from a model purely with vacancies on the Li site (of approximate composition $Li_{0.82}FeAs$); however, the different contrast between the scattering of Fe and Li by X-rays as compared to neutrons means that the two possible scenarios would be distinguishable by XRPD. We used joint refinements against NPD and synchrotron XRPD to satisfactorily resolve the structures of these compounds. We found that, while the structure could indeed be well modeled purely with Li-vacancies using NPD alone, this yielded a poorer fit to the corresponding XRPD data due to a lack of scattering from the 2*c* cation site, strongly indicating that Fe as well as Li is present on this site. This model, with $Li_{1-y}Fe_y$ on the 2*c* cation site, is also consistent with the chemical composition of the reactions that was carried out in sealed ampules: the high-quality diffraction data showed that the samples were phase pure (Figure 2), and the Li-vacancy-only model implies deficiency in the least volatile element, Fe, relative to the reaction mixture. The data showed no evidence for any measurable scattering from the interplanar tetrahedral site (2*b*: (0.75, 0.25, 0.5)), which it was suggested might be partially occupied by Li in ref 12. Furthermore, our refinements against both synchrotron XRPD data and NPD data indicated no deficiency on the As site within the experimental uncertainty, which is consistent with other structural reports of LiFeAs[10] and the density measurements of Juza and Langer.[12] We conclude on the basis of these experiments on several samples and from our own preliminary work that the samples described as $Li_{1.1-y}Fe_{1+y}As$ ($0 \le y \le 0.14$) by Juza and Langer[12] synthesized in glass ampules are systematically poorer in Li than they described perhaps because of lithium loss through reaction with the glass ampules.

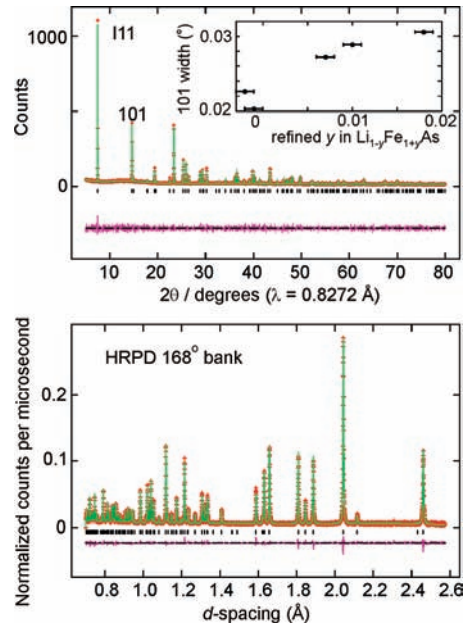

Figure 2. Results from the joint Rietveld refinement against I11 (upper) and HRPD (lower) data of the sample $Li_{1-y}Fe_{1+y}As$ with a nominal y of 0.02 (refined y of 0.01). The data (red crosses), fit (green line), difference (lower magenta line), and reflection positions are marked. The inset shows the width (fwhm derived from the GSAS refinements) in degrees 2θ of the 101 reflection measured on I11 using 0.8272 Å X-rays for several samples $Li_{1-y}Fe_{1+y}As$.

(20) Sonier, J. E.; Brewer, J. H.; Kiefl, R. F. *Rev. Mod. Phys.* **2000**, *72*, 769.

Table 1. Results of Joint XRPD−NPD Refinements on the Series $Li_{1-y}Fe_{1+y}As$

y (nominal)	0	0	0.01	0.02	0.03	0.04	0.05
y (refined)	−0.001(1)	0.004(1)	−0.002(1)	0.010(1)	0.018(1)	0.007(1)	0.040(1)
sample ID	MP127	MP98	MP142	MP143	MP144	MP145	MP129
radiation	combined neutron time-of-flight−synchrotron X-ray						
instruments	Polaris/I11	HRPD/I11	HRPD/I11	HRPD/I11	HRPD/I11	HRPD/I11	Polaris/I11
physical form	dark brown powder						
T/K	295	295	295	295	295	295	295
space group	*P*4/*nmm*						
a/Å	3.776840(2)	3.775280(2)	3.776047(2)	3.77377(5)	3.772561(5)	3.773962(3)	3.768861(2)
c/Å	6.35589(1)	6.35161(1)	6.35540(1)	6.34850(2)	6.34513(3)	6.34994(2)	6.33328(1)
V/Å^3	90.664(0)	90.528(0)	90.619(0)	90.411(1)	90.305(1)	90.441(0)	89.960(0)
Z	2	2	2	2	2	2	2
R_{wp}	0.0453		0.0386	0.0437	0.0401	0.0379	0.0563
R_{F2}	0.0664		0.0506	0.0499	0.0533	0.0420	0.0576
χ^2	4.035	4.929	5.686	4.244	7.169	5.441	3.127

We conducted joint XRPD−NPD refinements (Figure 2, Tables 1, S1, S2) using GSAS with the 2*c* cation site containing $Li_{1-y}Fe_y$ with y as a refined parameter. The lattice parameters were defined using the higher resolution synchrotron XRPD data collected with a calibrated wavelength on I11, and diffractometer constants were refined for the time-of-flight NPD data. Each sample measured on I11 exhibited a small degree of preferred orientation on account of the layered habit of the crystallites, and this was accounted for using a spherical harmonic function.

Figure 3 shows the unit cell volume plotted against the refined composition from the joint Rietveld refinement. This shows a clear decrease in the unit cell volume as y increases in $Li_{1-y}Fe_{1+y}As$ and Fe displaces Li from the 2*c* cation site. The refined value of y, shown in Figure 3 with an errorbar of one estimated standard deviation (esd) from GSAS, shows a smooth correlation with unit cell volume. The refined value of y is systematically smaller than the nominal value by about 0.01 (i.e., for the sample with a nominal y of 0.05, the refined value of y was 0.04), which is likely an artifact of the refinement. The esd's from GSAS are statistical uncertainties from the refinement and normally underestimate the true experimental uncertainty when performing the chemical analysis in this way, which is likely an order of magnitude larger in this case. Nevertheless, the consistency of the trend for several samples suggests that the unit cell volume is a useful sensitive measure of the composition in these compounds.

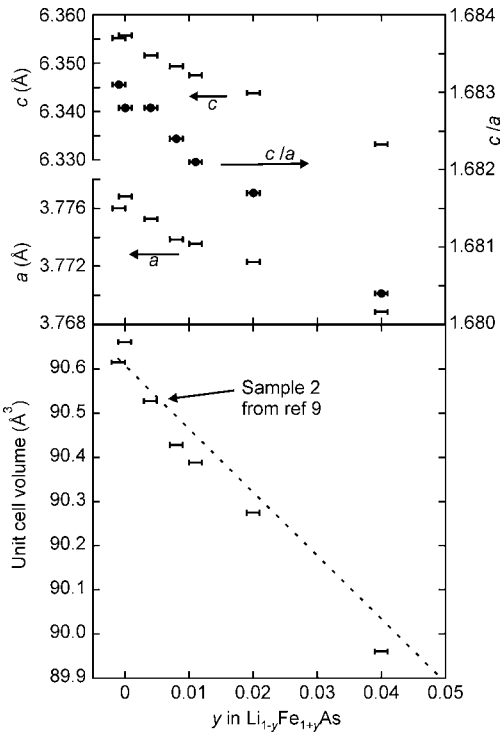

Figure 3. Lattice parameters derived from refinements against I11 data and their ratio (upper), and unit cell volume (lower) plotted against refined occupancy of the interlayer 2*c* site by Fe (from joint XRPD and NPD refinements). The error bars on the refined composition are 1 esd from GSAS. The uncertainties on the lattice parameters are smaller than the points. The dotted line shows the volume trend obtained by Juza and Langer against their nominal compositions (ref 12).

The dotted line in the plot in Figure 3 shows the trend in cell volume for the samples prepared by Juza and Langer.[12] In summary, our results are consistent with the results of ref 12 apart from a systematic difference in the Li content (i.e., the proposed 2*b* site appears unoccupied) and show that the unit cell volume is a useful measure of the composition of these $Li_{1-y}Fe_{1+y}As$ samples.

The analysis of the structural parameters (Figure 4, Tables S1, S2) obtained from the joint refinements shows that the 4-fold Li−As bond distance is almost invariant with y, but the interlayer Li−As distance decreases significantly as the 2*c* cation site becomes Fe-rich. This contraction of the $(Li,Fe)As_5$ coordination site (Figure 4) from an average Li−As distance of 2.737 Å in LiFeAs[9] is consistent with the shorter mean Fe(2*c*)−As distance of 2.554 Å in Fe_2As.[21]

As the Fe occupancy of the 2*c* cation site increases at the expense of the Li occupancy, we also see small changes in the shape of the $FeAs_4$ tetrahedra. The intraplane Fe−Fe distance (equal to $a/\sqrt{2}$) decreases by 0.2% as the refined value of y reaches 0.04, but the Fe−As distance shows no discernible variation (<0.02%) with composition given the experimental uncertainty in the refined distances. The As−Fe−As bond angle changes are consistent with this (Figure 4) and show that the FeAs layer becomes slightly more compressed in the basal plane as more Fe is accommodated in interlayer sites. These angle changes (and lattice parameter changes) match the types of changes that occur when pressure is applied; that is, the $FeAs_4$ tetrahedra become more distorted, and both lattice parameters contract. The structural changes between $y = 0$ and $y = 0.04$ correspond to those effected by the application of an hydrostatic pressure of about 1 GPa.[13]

Magnetic Susceptibility Measurements. As Fe is substituted for Li in LiFeAs, the superconducting properties change sharply. The superconducting transition temperature (T_c) follows an apparently linear decrease with decreasing unit cell volume down to a limit of ~90.42 Å^3, below which the system no longer

(21) Nuss, J.; Wedig, U.; Jansen, M. *Z. Kristallogr.* **2006**, *221*, 554.

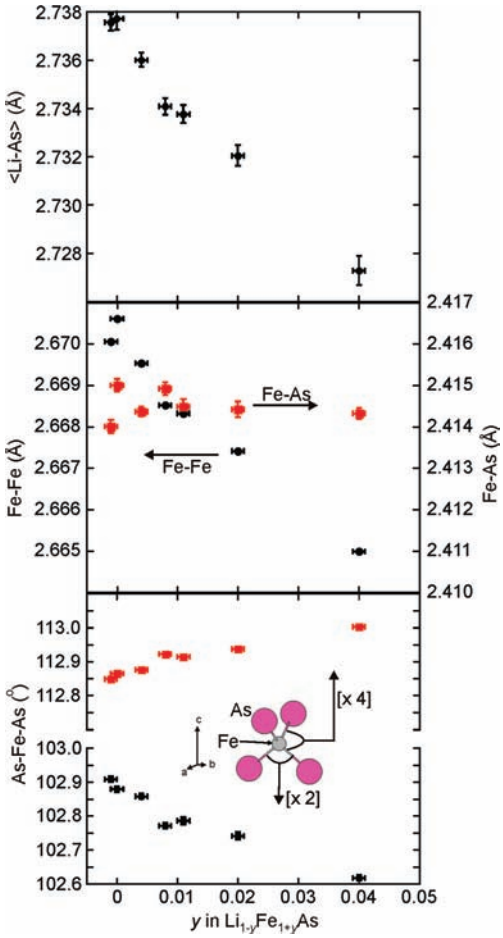

Figure 4. Trends in structural parameters with y in $Li_{1-y}Fe_{1+y}As$. Top: The weighted mean Li−As distance. Middle: The Fe−Fe and Fe−As distances shown on similar scales. Bottom: The As−Fe−As angles shown on similar scales.

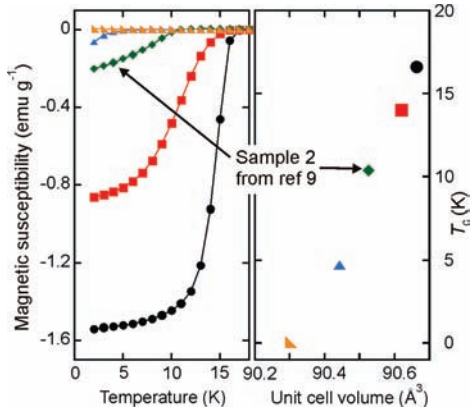

Figure 5. The evolution of the ZFC susceptibility (left) and T_c (right) with unit cell volume for samples $Li_{1-y}Fe_{1+y}As$.

supports superconductivity. We have shown above that the unit cell volume is proportional to y. The trend in decreasing T_c is also accompanied by a decrease in the superconducting volume fraction, illustrated in Figure 5. The superconducting transition also becomes broader as the Fe(2*c*) content increases. This suggests that the doping of Fe onto the Li site is not perfectly homogeneous so that the doped materials may contain nonsuperconducting regions that are Fe-rich and superconducting regions with a range of T_c's that are poorer in Fe. Inspection of the diffraction patterns obtained from I11 clearly shows that the Bragg peaks broaden significantly with increasing y, increasing by 50% in the range $0 \le y$(refined) ≤ 0.02 as shown in Figure 2. Samples with unit cell volumes below 90.4 Å exhibit non-Curie−Weiss-like temperature-dependent paramagnetism, which we have not analyzed. The extreme sensitivity of superconductivity in LiFeAs to substitution of Li by Fe is quantitatively similar to that exhibited by the $Fe_{1+x}Se$ system.[22] FeSe with the PbO structure is isostructural with the FeAs portion of the LiFeAs structure. FeSe can accommodate a small amount of excess Fe on the 2*c* sites occupied by Li in LiFeAs. $Fe_{1.01}Se$ is a superconductor, while the incorporation of just 2% of additional Fe on this site to form $Fe_{1.03}Se$ destroys the superconducting state.[22] However, we should note that in LiFeAs superconductivity is suppressed linearly by the application of pressure,[13,14] while in β-FeSe, dT_c/dP is initially positive and T_c reaches a maximum of 37 K at 7 GPa.[23,24]

Our structural investigations described above suggest that the substitution of Fe for Li on the 2*c* cation site corresponds to the application of a hydrostatic pressure of 1 GPa for $y \approx 0.05$ in $Li_{1-y}Fe_yAs$. However, superconductivity is completely quenched when y reaches 0.02, while the T_c in LiFeAs is lowered by only about 2 K on application of a hydrostatic pressure of 1 GPa.[13] So the substitution of Fe for Li on the 2*c* cation site is much more effective at suppressing superconductivity than the application of hydrostatic pressure. In our earlier reports on LiFeAs,[9,25] we reported two samples with different T_c's, which were otherwise difficult to distinguish on the basis of composition or structure. Our analysis of the relationship between unit cell volume, composition, and superconductivity using further samples close in composition to LiFeAs allows us to conclude that "sample 2" reported in our earlier papers[9,25] with a low T_c contains an estimated 1% Fe on the Li site.

Co-Doped and Ni-Doped LiFeAs. Structural Characterization. Structural characterization of the Co-doped series was carried out primarily by synchrotron XRPD using I11 and ID31, with two samples ($x = 0.15, 0.2$) also measured by NPD on Polaris. The Ni-doped series was characterized by NPD using Polaris (ISIS, UK), and samples of composition $x = 0.01, 0.015$, and 0.025 were measured by XRPD on I11. Both series were modeled with Co or Ni sharing the Fe site (i.e., the 2*a* site; see Figure 1). X-ray scattering amplitudes are very similar for these metals giving very poor contrast by XRPD, while the neutron scattering lengths of Fe and Ni are also similar (Fe, 9.54 fm; Ni, 10.3 fm), which precludes any reliable refinement of Fe/Ni occupancy from experiments on this series. There is, however, very good contrast between Fe and Co using neutrons (Co: 2.45 fm). Measurement of $LiFe_{0.85}Co_{0.15}As$ (Figure 6) and $LiFe_{0.80}Co_{0.20}As$ by NPD produced refined compositions of $LiFe_{0.857(3)}Co_{0.143(3)}As$ and $LiFe_{0.812(1)}Co_{0.188(1)}As$ (where the esd's are the statistical uncertainties in the refinements derived from GSAS) consistent with the nominal composition and lack of impurity phases within the experimental uncertainty. Refinement

(22) McQueen, T. M.; Huang, Q.; Ksenofontov, V.; Felser, C.; Xu, Q.; Zandbergen, H.; Hor, Y. S.; Allred, J.; Williams, A. J.; Qu, Q.; Checkelsky, J.; Ong, N. P.; Cava, R. J. *Phys. Rev. B* **2009**, *79*, 014522.
(23) Margadonna, S.; Takabayashi, Y.; Ohishi, Y.; Mizuguchi, Y.; Takano, Y.; Kagayama, T.; Nakagawa, T.; Takata, M.; Prassides, K. *Phys. Rev. B* **2009**, *80*, 064506.
(24) Medvedev, S.; McQueen, T. M.; Troyan, I. A.; Palasyuk, T.; Eremets, M. I.; Cava, R. J.; Naghavi, S.; Casper, F.; Ksenofontov, V.; Wortmann, G.; Felser, C. *Nat. Mater.* **2009**, *8*, 630.
(25) Pratt, F. L.; Baker, P. J.; Blundell, S. J.; Lancaster, T.; Lewtas, H. J.; Adamson, P.; Pitcher, M. J.; Parker, D. R.; Clarke, S. J. *Phys. Rev. B* **2009**, *79*, 052508.

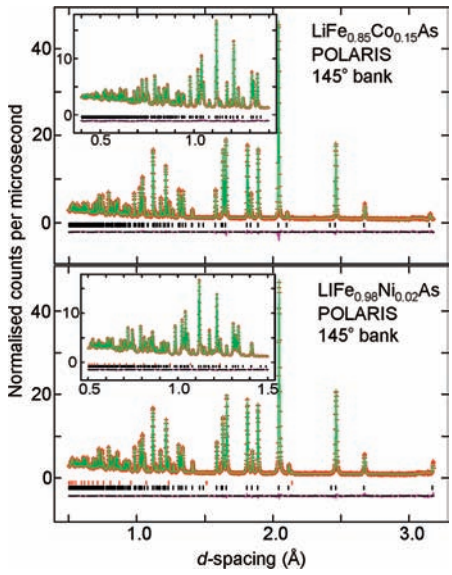

Figure 6. Rietveld refinements against Polaris NPD data for Co and Ni-doped LiFeAs derivatives. The data (red crosses), fit (green line), difference (lower magenta line), and reflection positions are marked. The upper set of red reflection markers below the $LiFe_{0.98}Ni_{0.02}As$ pattern are from the vanadium sample container.

results for these compounds are summarized in Tables 2 and 3, and refined parameters are tabulated in Tables S3−S7.

Figure 7 shows plots of lattice parameters and unit cell volume versus composition for the Co-doped and Ni-doped series. The parameters are shown normalized to their values at $x = 0$. As x increases in $LiFe_{1-x}Co_xAs$ and $LiFe_{1-x}Ni_xAs$, the basal lattice parameter, a ($= \sqrt{2} \times$ Fe−Fe) increases linearly, while the c parameter decreases more sharply leading to a decrease in the unit cell volume. The rates of change in the lattice parameters with x are similar for the Ni-doped and Co-doped members as emphasized in the plot of c/a ratio versus composition for both series (Figure 7).

Note that the decrease in unit cell volume in these Co- and Ni-doped compounds (which is depicted in Figure 7) is much less rapid with x than is the contraction with increasing y in the $Li_{1-y}Fe_{1+y}As$ series considered above (in which both a and c decrease with increasing y). In Figure 7, the green dashed line represents the evolution in cell volume shown in Figure 3. These changes on Co- or Ni-doping are consistent with the similar Co−Se and Ni−Se distances in the NiAs-type binary monoselenides (2.48 and 2.50 Å, respectively),[26] which are shorter than the Fe−Se distances in FeSe (2.57 Å).[27]

Figure 8 shows the evolution in structural parameters on Co or Ni doping. On adding electrons to the system and replacing some of the Fe by the smaller Co or Ni, the Fe−Fe distance increases and the Fe−As distance decreases. The $FeAs_4$ tetrahedra therefore become slightly less distorted. These changes are in contrast to the effect of substituting Li by Fe (in which the Fe−Fe distance contracts and the Fe−As distance is invariant (Figure 4)) and in contrast to the application of hydrostatic pressure.

During the course of this work, in attempts to synthesize large samples of $LiFe_{1-x}Co_xAs$, we produced phases with nominal values of x of 0.025, 0.05, and 0.1 with anomalously small unit cell volumes, which contained impurities (e.g., FeAs). These samples do not undergo a superconducting transition and appear to have all of the characteristics of the iron-rich $Li_{1-y}Fe_{1+y}As$-type materials discussed in the previous section. The reduced cell volumes and the properties are in these cases consistent with the substitution of 2−3% of the Li by transition metals on the 2c cation site, which, as we have shown above, is sufficient to destroy the superconducting state.

Magnetic Susceptibility Measurements. All samples were studied by dc-SQUID magnetometry. In both the Co- and the Ni-doped series, the superconducting transition temperature is suppressed and the magnetometry measurements suggest a decrease in the superconducting volume fraction as x increases (Figure 9). T_c shows a linear decrease with increasing electron count (Figure 10), which appears to be independent of the identity of the dopant (i.e., compounds $LiFe_{1-x}Co_xAs$ have magnetic properties similar to those of $LiFe_{1-x/2}Ni_{x/2}As$). This is consistent with our studies of the effect of Co- and Ni-doping on the isostructural NaFeAs.[16] We observed the lowest T_c at ~3.6 K in the 5% Ni-doped sample, and superconductivity is suppressed at a linear rate of about 10 K per 0.1 electrons added per formula unit. For samples with higher electron counts, superconductivity is replaced by complex paramagnetic behavior, with evidence for low temperature magnetic transitions and some evidence for glassy behavior, which requires further investigation. This suppression of superconductivity by electron-doping in LiFeAs is quite different from that observed in the NaFeAs derivatives, where the superconducting properties are enhanced at small doping levels (up to $0.05e^-$ per formula unit) but are ultimately quenched at higher doping levels (above $0.10e^-$ per formula unit).[16] Figure 9 shows that on doping the superconducting volume fractions decrease, and some of the transitions are apparently broadened. This broadening in the superconducting transition may be due to compositional inhomogeneity within the samples.

Muon-Spin Rotation Measurements. Two of the most important parameters used to characterize a superconductor are the critical temperature T_c and the superfluid stiffness ρ_s, and the relationship between them yields important information concerning the interplay of pairing and electromagnetic screening within the superconducting state. In many superconductors, including the iron pnictides,[28,29] these parameters have been shown to obey a linear scaling relation (the so-called "Uemura scaling").[30,31] Examination of the scaling relation for different series of superconductors within a particular class may give some insight into their underlying behavior. For example, electron-doped and hole-doped cuprate superconductors display quite different Uemura scaling behavior with a much stiffer superfluid evident for the electron-doped materials as compared to the hole-doped materials. As noted previously,[9,13] LiFeAs is structurally quite different from the other iron pnictide superconductors: the $FeAs_4$ tetrahedra are highly compressed in the basal plane resulting in shorter Fe−Fe distances than in the

(26) Komarek, K. L.; Wessely, K. *Monatsh. Chem.* **1972**, *103*, 896.
(27) Franz, E. D. *Neues Jahrb. Mineral., Monatsh.* **1970**, *1970*, 147–157.
(28) Luetkens, H.; Klauss, H.-H.; Khasanov, R.; Amato, A.; Klingeler, R.; Hellmann, I.; Leps, N.; Kondrat, A.; Hess, C.; Köhler, A.; Behr, G.; Werner, J.; Büchner, B. *Phys. Rev. Lett.* **2008**, *101*, 097009.
(29) Drew, A. J.; Pratt, F. L.; Lancaster, T.; Blundell, S. J.; Baker, P. J.; Liu, R. H.; Wu, G.; Chen, X. H.; Watanabe, I.; Malik, V. K.; Dubroka, A.; Kim, K. W.; Rössle, M.; Bernhard, C. *Phys. Rev. Lett.* **2008**, *101*, 097010.
(30) Uemura, Y. J.; et al. *Phys. Rev. Lett.* **1989**, *62*, 2317.
(31) Uemura, Y. J.; Le, L. P.; Luke, G. M.; Sternlieb, B. J.; Wu, W. D.; Brewer, J. H.; Riseman, T. M.; Seaman, C. L.; Maple, M. B.; Ishikawa, M.; Hinks, D. G.; Jorgensen, J. D.; Saito, G.; Yamochi, H. *Phys. Rev. Lett.* **1991**, *66*, 2665.

Table 2. Results of PXRD Refinements and Joint PXRD−NPD Refinements on the Series $LiFe_{1-x}Co_xAs$

x (nominal)	0	0.025	0.05	0.075	0.1	0.15	0.2
x (refined)		a	a	a	a	0.143(3)	0.188(1)
sample ID	MP127	MP151	MP152	MP171	WTT9	MP161	WTT19
instruments	I11+Polaris	I11	I11	I11	ID31	I11+Polaris	ID31+Polaris
physical form				dark brown powder			
T/K	295	295	295	295	295	295	295
space group				*P*4/*nmm*			
a/Å	3.776840(2)	3.777858(4)	3.778905(4)	3.779206(4)	3.78105(1)	3.781453(1)	3.783230(7)
c/Å	6.35589(1)	6.35021(1)	6.34237(1)	6.33216(1)	6.32658(3)	6.30989(1)	6.29562(2)
V/Å^3	90.664(0)	90.632(0)	90.570(0)	90.438(0)	90.447(1)	90.228(0)	90.108(0)
Z	2	2	2	2	2	2	2
R_{wp}	0.0453	0.0558	0.0763	0.0776	0.1055	0.0580	0.0479
R_{F2}	0.0664	0.0647	0.0967	0.0544	0.0487	0.0608	0.0395
χ^2	4.035	6.844	6.922	5.630	1.790	6.407	1.867

[a] Not refined (XRPD data only).

Table 3. Results of NPD Refinements on the Series $LiFe_{1-x}Ni_xAs$

x (nominal)	0	0.005	0.015	0.02	0.025	0.05	0.1	0.2
sample ID	MP127	MP159	MP157	MP158	MP155	MP160	WTT31	WTT42
instruments	Polaris/I11	Polaris				Polaris		
T/K				295				
space group				*P*4/*nmm*				
a/Å	3.776840(2)	3.77562(2)	3.77690(2)	3.77732(2)	3.7777(2)	3.77931(2)	3.78408(3)	3.78686(4)
c/Å	6.35589(1)	6.35269(4)	6.35051(4)	6.34849(5)	6.34710(4)	6.33938(4)	6.32770(5)	6.30122(7)
V/Å^3	90.664(0)	90.559(2)	90.590(1)	90.581(2)	90.579(2)	90.547(1)	90.608(2)	90.361(2)
Z	2	2	2	2	2	2	2	2
R_{wp}	0.0453	0.0223	0.0218	0.0221	0.0250	0.0217	0.0234	0.0217
R_{F2}	0.0664	0.0449	0.0472	0.0474	0.0465	0.0494	0.0541	0.0688
χ^2	4.035	1.565	1.582	1.584	2.044	2.089	0.9778	0.8609

isostructural NaFeAs-derivatives, the "1111" compounds and the "122" compounds, all of which have $FeAs_4$ tetrahedra that are close to regular in shape. Our earlier measurements[25] show that the superfluid stiffness of LiFeAs in relation to its T_c is enhanced as compared to other pnictide superconductors.[16,28]

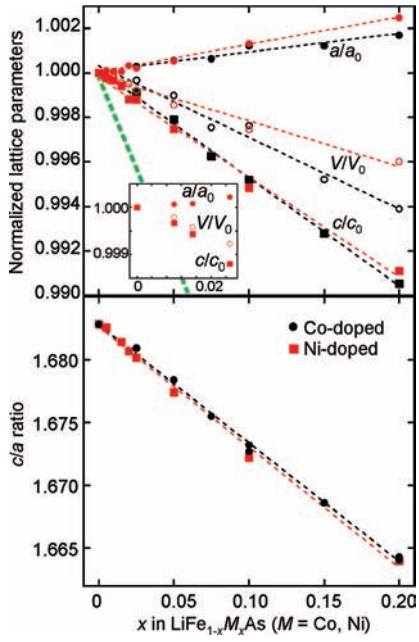

Figure 7. Top: The evolution of lattice parameters a (●) and c (■) and unit cell volume (○) with doping in $LiFe_{1-x}M_xAs$ for M = Co (black symbols) and Ni (red symbols). The values are normalized against those of LiFeAs. The inset shows the behavior for Ni-doped samples at low doping levels as measured on I11. The green dashed line indicates the trend in volume with y for the $Li_{1-y}Fe_{1+y}As$ samples (Figure 3). Bottom: The evolution of the c/a ratio for the two series. In all cases, the dotted lines are linear best fits to the data.

The present experiment aimed to investigate the behavior over a wider range of compositions $LiFe_{1-x}M_xAs$ (M = Co, Ni) to enable a clearer comparison between the LiFeAs-derivatives and other superconductors.

Figure 11 shows typical TF-μSR spectra for $LiFe_{0.99}Ni_{0.01}As$, both above and below T_c. The damping of the oscillations is well described by a Gaussian envelope, the decay rate of which is related to the width (B_{rms}) of the field distribution within the

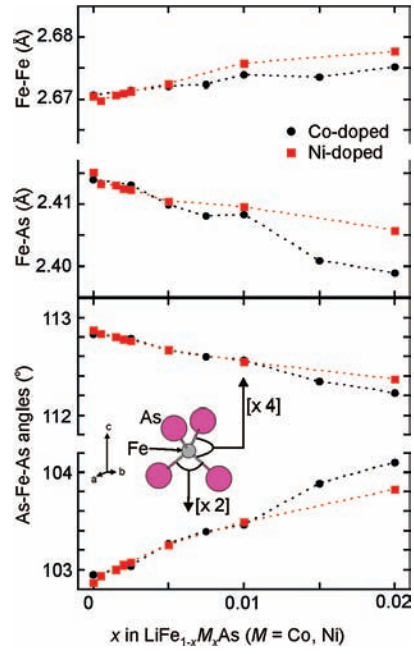

Figure 8. The trends in distances and angles on doping LiFeAs with Co (●) or Ni (red ■). The distances and angles are both shown on similar scales. Lines are guides to the eye.

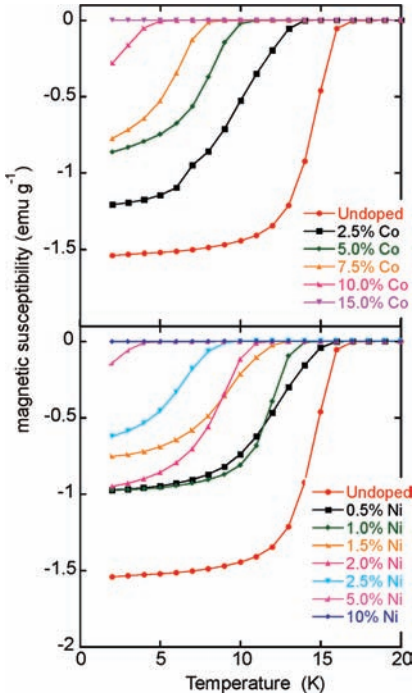

Figure 9. ZFC magnetic susceptibilities for $LiFe_{1-x}Co_xAs$ and $LiFe_{1-x}Ni_xAs$ samples.

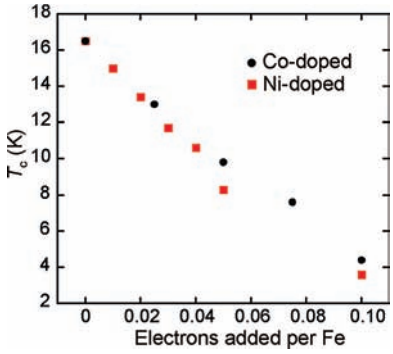

Figure 10. The dependence of T_c on electron count in $LiFe_{1-x}Co_xAs$ and $LiFe_{1-x}Ni_xAs$ samples.

sample. Below T_c, the broadening increases significantly due to the dephasing contributions from the vortex lattice.

B_{rms} is determined as a function of temperature (Figure 12), and the temperature dependence is fitted to the following empirical relation:

$$B_{rms} = \left[B_0\left(1 - \left(\frac{T}{T_c}\right)^{\alpha}\right)^2 + B_g^2\right]^{1/2} \quad (2)$$

where B_g represents the contribution of randomly orientated nuclear moments near the muon site and is independent of the presence of superconductivity.

This treatment was found to account well for the behavior of B_{rms} with temperature for the Co- or Ni-doped samples. However, we note that the data for undoped LiFeAs could not be fitted in this way, reflecting the fact that superconductivity in undoped LiFeAs is unusual, perhaps due to its proximity to a magnetic instability.[25] Doping seems to establish a more conventional superconducting state. Fitted values for T_c, α, B_g, and B_0 are shown in Table 4. B_0 is the zero temperature contribution to B_{rms} due to the presence of a vortex lattice and

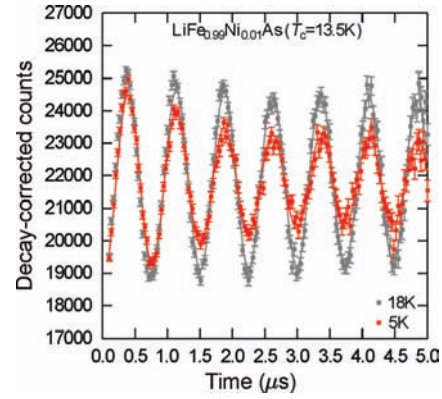

Figure 11. TF-μSR spectra for $LiFe_{0.99}Ni_{0.01}As$, which represents a typical sample. Decay-corrected count against time is shown both above and below T_c in an applied transverse field B_{app} of 10 mT.

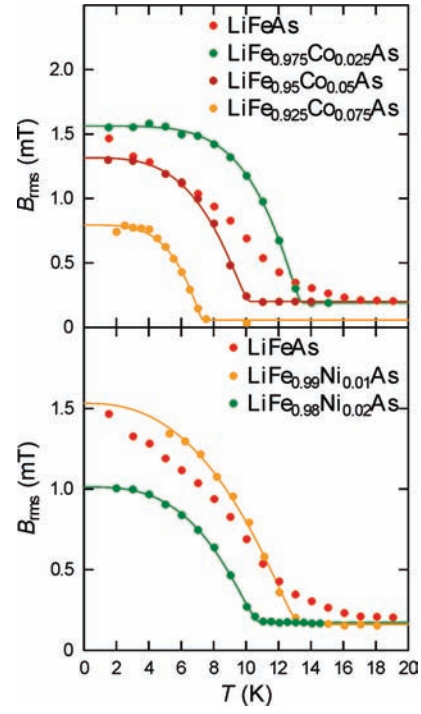

Figure 12. Variation of B_{rms} with T for $LiFe_{1-x}M_xAs$ where M = Co (upper) or Ni (lower). All measurements were carried out in an applied field of 10 mT. The data for stoichiometric LiFeAs are those of "sample 1" in ref 25. The lines are fits to eq 2.

is related to the in-plane penetration depth λ_{ab} for a powder sample:[32]

$$\lambda_{ab}^2 = \left(\frac{0.00371}{3}\right)^{1/2}\frac{\phi_0}{B_0} \quad (3)$$

where ϕ_0 is the flux quantum.

An Uemura plot of λ_{ab}^{-2} against T_c shows how T_c scales with the superfluid stiffness ρ_s ($\rho_s/c = \lambda_{ab}^{-2}$). The behavior of these LiFeAs-derivatives is compared to that of several different series of superconductor in Figure 13. It is clear that the behavior of LiFeAs-derived compounds is markedly different from that of other pnictides, including the isostructural NaFeAs-derivatives and the "1111" and "122" classes. Most of the pnictides exhibit

(32) Fesenko, V. I.; Gorbunov, V. N.; Smilga, V. P. *Physica C* **1991**, *176*, 551.

Table 4. Parameters Obtained from Fits to the Temperature-Dependent Transverse-Field Muon-Spin Rotation Data

sample	B_0 (mT)[a]	T_c (K)[a]	α[a]	B_g (mT)[a]	λ_{ab}^{-2} (μm^{-2})[b]
$LiFe_{0.975}Co_{0.025}As$	1.54(6)	13.52 (1)	4.7(1)	0.118(2)	21.2(1)
$LiFe_{0.95}Co_{0.05}As$	1.27(4)	10.00(1)	4.2(6)	0.204(5)	17.4(6)
$LiFe_{0.925}Co_{0.075}As$	0.79(1)	7.35(5)	3.9(3)	0.060(1)	10.9(2)
$LiFe_{0.99}Ni_{0.01}As$	1.52(7)	13.41(8)	2.4(2)	0.161(5)	21.0(9)
$LiFe_{0.98}Ni_{0.02}As$	1.00(1)	10.93(4)	3.0(1)	0.173(2)	13.4(2)

[a] B_0, T_c, α, and B_g were obtained by fitting the temperature dependence of B_{rms} to eq 2. [b] The inverse squared penetration depth λ_{ab}^{-2} was obtained from eq 3.

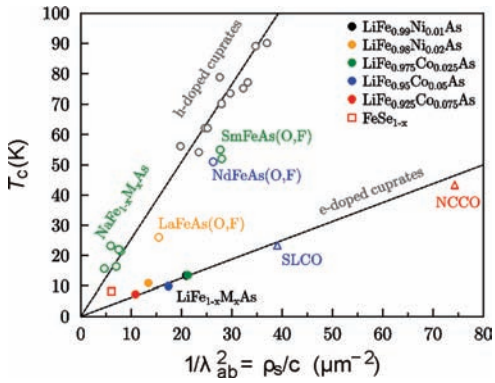

Figure 13. Uemura plot for $LiFe_{1-x}M_xAs$, where M = Co, Ni. Also shown for comparison are previously obtained data on hole-doped cuprates,[36] other pnictides including the Na-based materials isostructural with LiFeAs,[16,28,29] FeSe,[33] and the electron-doped cuprates $Nd_{1.85}Ce_{0.15}CuO_4$ (NCCO)[37] and $Sr_{0.9}La_{0.1}CuO_2$ (SLCO).[38]

behavior more similar to the hole-doped cuprates, but LiFeAs-derivatives resemble much more closely the electron-doped cuprates. The location of FeSe on this plot seems to suggest intermediate behavior between LiFeAs and the other pnictides, although the limited data are not inconsistent with the other similarities, which we have noted with LiFeAs; the μSR data on FeSe are discussed in more detail elsewhere.[33] Recent investigations of LiFeAs using small-angle neutron scattering (SANS)[34] and angle-resolved photoemission spectroscopy (ARPES)[34,35] have been used to probe the superconducting properties and Fermi surface of LiFeAs. The SANS measurements[34] produced a value of the in-plane penetration depth, λ_{ab}, of 210 $\pm$ 20 nm, in good agreement with our μSR measurements,[25] and an in-plane coherence length of 7 $\pm$ 2 nm.

Comparison of LiFeAs to Related Systems. LaFeAsO, AFe_2As_2 (A = Ca, Sr, Ba), and NaFeAs are isoelectronic with LiFeAs, and these compounds are all itinerant antiferromagnets at ambient pressure in their undoped states. They can be driven into the superconducting regime by hole or electron doping or by the application of pressure. The magnetic ordering results from a Fermi surface instability, which is driven by nesting. LiFeAs, by contrast, is a superconductor in its undoped form, and the application of pressure or doping serves always to suppress superconductivity. The Fe−Fe distance of 2.67 Å in LiFeAs is 4.4% shorter than the mean Fe−Fe distance of about 2.79 Å in the other iron arsenide superconductors, which have Fe−Fe distances that have a span of only 2.5% around this mean. The effect of this structural difference on the band structure is presumably what accounts for the lack of Fermi surface nesting revealed by ARPES measurements.[39] In turn, this lack of Fermi surface nesting means that in undoped LiFeAs the magnetic instability that is found in the other isoelectronic (i.e., undoped) iron arsenides does not compete successfully against superconductivity.

The temperature dependence of the penetration depth determined by SANS measurements[34] was only consistent with a single nodeless superconducting gap of 3.0 $\pm$ 0.2 meV, which is consistent with weak pairing within the framework of the BCS theory. The ARPES measurements[39] furthermore suggest that LiFeAs has an enhanced density of states at E_F, which results from a van Hove singularity. These observations lead to the suggestion that LiFeAs may be a conventional phonon-mediated superconductor with an enhanced density of states at E_F accounting for the high T_c and different from the other pnictides. This view is supported by measurements of the quasiparticle lifetime using further ARPES measurements.[35] However, antiferromagnetic fluctuations have been used to account for the ^{75}As NMR spectra of LiFeAs,[40] so one cannot rule out the notion that spin fluctuations play a role in coupling the superconducting pairs in LiFeAs. Recent susceptibility measurements also suggest two-gap behavior[41] rather than the single-gap behavior suggested by SANS measurements.[34] Further experiments are clearly required to fully resolve the behavior of LiFeAs.

Conclusions

In the iron pnictide superconductors, there is well-documented competition between magnetic order and superconductivity, which is dependent on doping. LiFeAs is unusual as compared to the "1111" and "122" iron arsenides and even the isostructural "111" compound NaFeAs, because the stoichiometric material does not exhibit static magnetic order, but is instead superconducting. The ultimate origin of this may be that the Fe−Fe distance in LiFeAs is much shorter than that in the other arsenides. Indeed, the short Fe−Fe distance and the occurrence of superconductivity in the stoichiometric phase rather than magnetic order make LiFeAs resemble layered, tetragonal β-FeSe much more than the other arsenides, although there are also clear differences between LiFeAs and β-FeSe, particularly in the response of superconductivity to applied hydrostatic

(33) Amato, A.; Khasanov, R.; Luetkens, H.; Klauss, H.-H. *Physica C* **2009**, *469*, 606.
(34) Inosov, D. S.; et al. *Phys. Rev. Lett.* **2010**, *104*, 187001.
(35) Kordyuk, A. A.; Zaboloynyy, V. B.; Evtushinsky, D. V.; Kim, T. K.; Morozov, I. V.; Follath, R.; Behr, G.; Büchner, B.; Borisenko, S. V., arXiv:1002.3149.
(36) Uemura, Y. J. *Physica B* **2006**, *374*, 1.
(37) Homes, C. C.; Clayman, B. P.; Peng, J. L.; Greene, R. L. *Phys. Rev. B* **1997**, *56*, 5525.
(38) Shengelaya, A.; Khasanov, R.; Eshchenko, D. G.; Di Castro, D.; Savić, I. M.; Park, M. S.; Kim, K. H.; Lee, S.-I.; Müller, K. A.; Keller, H. *Phys. Rev. Lett.* **2005**, *94*, 127001.
(39) Borisenko, S. V.; Zabolotnyy, V. B.; Evtushinsky, D. V.; Kim, T. K.; Morozov, I. V.; Yaresko, N.; Kordyuk, A. A.; Behr, G.; Vasiliev, A.; Follath, R.; Büchner, B., arXiv:1001.1147.
(40) Jeglič, P.; Potočnik, A.; Klanjšek, M.; Bobnar, M.; Jagodič, M.; Koch, K.; Rosner, H.; Margadonna, S.; Lv, B.; Guloy, A. M.; Arèon, D. *Phys. Rev. B* **2010**, *81*, 140511(R).
(41) Sasmal, K. Lv, B.; Tang, Z.; Wei, F. Y.; Xue, Y. Y.; Guloy, A. M.; Chu, C. W., arXiv:1004.1387.

pressure noted above.[23,24] Normally in the arsenides, electron or hole doping or the application of hydrostatic pressure is required to drive the stoichiometric systems away from magnetic order and into the superconducting regime. In contrast, the electron doping on the Fe site of LiFeAs by Co or Ni, which we report here, in common with the application of hydrostatic pressure, serves only to suppress superconductivity. In principle, hole doping in LiFeAs could be achieved by Li deficiency. An early report[11] suggested that Li-deficient materials (i.e., $Li_{1-y}FeAs$ with Li vacancies, but no Fe on the 2*c* cation site) were attainable and were superconducting, but these conclusions have not been substantiated by any later study. The investigations reported here show that the superconducting state is extremely sensitive to nonstoichiometry in the form of substitution of some of the Li ions on the 2*c* site by Fe in Li-poor/Fe-rich compositions $Li_{1-y}Fe_{1+y}As$. The use of high-quality synchrotron and neutron powder diffraction data enabled a correlation between unit cell volume and refined composition to be used to show that a substitution of less than 2% of the Li by Fe is sufficient to destroy the superconducting state in LiFeAs, and accounted for an earlier observation that LiFeAs samples that were indistinguishable compositionally and structurally by isolated measurements displayed very different superconducting properties.[9,25] With respect to the response to this nonstoichiometry, LiFeAs bears quantitative comparison with the isoelectronic FeSe in addition to the other similarities with the FeSe system described above. Substitutions on the Fe site in LiFeAs are much less disruptive of either the crystal structure or the superconducting properties, although the substitution of Fe by Co or Ni only serves to decrease T_c and the superfluid stiffness, eventually destroying the superconducting state when about 0.1 electrons per formula unit have been added using either Co or Ni as the dopant. Electron count seems to be a key parameter in controlling the superconductivity: Co- and Ni-doping produce similar structural responses per dopant atom, but the suppression of T_c with x in $LiFe_{1-x}M_xAs$ is twice as rapid when M = Ni than when M = Co. The μSR measurements reveal that in LiFeAs the superfluid is much stiffer than would be expected on the basis of the expectations of the other classes of iron pnictide superconductor. There is now evidence from several sources that LiFeAs is sufficiently different in behavior from the other iron arsenides that a full understanding of this compound is important for testing theories of superconductivity in the entire class.

Acknowledgment. We are grateful to Dr. R. I. Smith and Dr. K. S. Knight (ISIS facility) for assistance on Polaris and HRPD; Dr. C. C. Tang, Dr. S. P. Thompson, and Dr. J. Parker for assistance on I11; and Dr. I. Margiolaki and Dr. A. N. Fitch for assistance on ID31. The μSR work was carried out at both the ISIS facility, Didcot, UK, and the SμS facility, Villigen, CH. We acknowledge the financial support of the EPSRC (UK).

Supporting Information Available: Lists of refinement results and structural parameters together with field-dependent μSR data and complete refs 30 and 34. This material is available free of charge via the Internet at http://pubs.acs.org.

JA103196C